Journal of Neuroimmune Pharmacology (2019) 14:251–262
https://doi.org/10.1007/s11481-018-9817-2

ORIGINAL ARTICLE

Age-Induced Spatial Memory Deficits in Rats Are Correlated with Specific Brain Region Alterations in Microglial Morphology and Gene Expression

Shai Shoham[1] · Michal Linial[2] · Marta Weinstock[1]

Received: 23 July 2018 / Accepted: 12 October 2018 / Published online: 20 October 2018

Abstract

Effect of age and ladostigil treatment (1 mg/kg/day), given for 6 months to 16 month old rats, was investigated on microglial morphology in brain regions associated with control of spatial learning. This was assessed in the Morris water maze (MWM). Microglial morphology was assessed with diaminobenzidine and fluorescent staining with Iba1 and CD11b in these brain regions. Aging did not change the number of microglia in the parietal cortex (PC) or hippocampal CA1 region (CA1-HC), but decreased microglial process tips in the CA1-HC, increased the area fraction stained by CD11b and number of bulbs on processes in PC and CA1-HC and thickness of microglial processes in corpus callosum (CC) and fornix (Fx). Performance in MWM (distance swam to escape platform) was negatively correlated with number of bulbs in PC and thickness of process in CC, and positively correlated with number of process tips in CA1-HC. Aging increased expression of MHC class II genes and others associated with motility and membrane adhesion in the PC and hippocampus, but Adora2a (Adenosine A2a receptor), only in hippocampus. Age-related increase in the number of bulbs and expression of inflammatory genes was prevented by ladostigil in PC. In the CA1-HC, ladostigil increased the number of process tips and prevented the increase in expression of Adora2a and genes regulating ion channels. Ladostigil also decreased thickening of the processes in CC and Fx. The data show brain region-specific relations induced by age in spatial learning, microglial morphology and associated genes and their response to ladostigil treatment.

Keywords Hippocampus · KEGG pathway · Microglial morphology · Parietal cortex · RNA-Seq

Abbreviations

CA1-HC	hippocampal CA1 region
CC	corpus callosum
DAB	diaminobenzidine
FPKM	Fragments per kilobase million
Fx	fornix
HC	hippocampus
Iba1	Ionized calcium binding adaptor molecule 1 protein
MWM	Morris water maze
PC	parietal cortex

✉ Marta Weinstock
martar@ekmd.huji.ac.il

[1] The Institute for Drug Research, School of Pharmacy, The Hebrew University of Jerusalem, Jerusalem, Israel

[2] Department of Biological Chemistry, Life Science Institute, The Hebrew University of Jerusalem, 91904 Jerusalem, Israel

Introduction

An age-related decline in cognitive function, including spatial learning and memory (Light and Zelinsky 1983; Pezdek 1983; Petersen et al. 1992; Gallagher and Nicolle 1993; Ingram et al. 1994) is common to all species studied. Such deficits in spatial learning and memory are associated with cell damage that results from oxidative stress, prolonged microglial activation and release of pro-inflammatory cytokines (Bickford et al. 2017). Microglia of aged rodents and humans have a lower threshold for activation (Perry et al. 2010) and a higher expression than that found in younger ones of genes of inflammatory markers of the major histocompatibility complex (MHC class II) immune response pathway and pro-inflammatory cytokines like TNF-α and IL-1β (Wong 2013).

Spatial learning and memory require the integration of information between the hippocampus (HC) and several brain regions including the parietal cortex (PC) (Save and Poucet 2009; Li et al. 2014; Whitlock 2014), fornix (Fx) (Aggleton et al. 2009; Hescham et al. 2013) and corpus callosum (CC)

(Bettcher et al. 2014; Li et al. 2014). Disruption in the function of any of these regions can impair spatial memory (Vann et al. 2011; Albasser et al. 2013; Conejo et al. 2013). However, most studies that investigated a relation between memory impairment and alterations in microglial activity and/or morphology in aged rats were confined to the HC (Jacobson et al. 2008; VanGuilder et al. 2011; Lana et al. 2016;). Although an increase was found in the expression of neuroinflammatory signaling transcripts and Iba1 protein in hippocampal sub-regions in 24 month old Fischer rats, the expression of these transcripts did not differ between those with impaired and intact memory (Van Guilder et al., 2011). Moreover, in the HC, there do not appear to be any reports of a relation between the magnitude of a change in microglial morphology or activity and that in spatial memory.

Relatively few studies have been reported on spatial learning and memory in male rats of different ages. Like that cited above, most of them were performed in inbred strains like Fisher 344 and its hybrids. The Fisher344/Brown Norway F1 hybrid was developed by the National Institute on Aging (NIA) as a genetically defined rat model with an improved health profile at older ages. They have a longer lifespan and a delayed onset of age-associated pathologies (Spangler et al., 1994; Turturro et al. 1999), but these may not be typical of age related changes in other strains. Even in this hybrid strain, the onset of spatial memory impairment is very variable and may be as early as 18, or as late as 31 months of age (Hebda-Bauer et al. 1999; McQuail and Nicholl 2015). In Sprague Dawley and Wistar Kyoto rat strains, spatial learning in the Morris water maze (MWM) is largely intact until 18 months of age, and at this age, rats appear to use a different strategy to find the escape platform (Wyss et al. 2000).

Wistar rats have a significant increase in the expression of genes that denote neuroinflammation (CD86, CD40 and ICAM), together with that of pro-inflammatory cytokines, IL-1β, IFNγ and IL-18 at 15 months of age (Griffin et al. 2006). These rats also show a reduction in hippocampal LTP, indicating that inflammation precedes and probably contributes to spatial memory impairment. However, we are unaware of reports of spatial learning or measures of microglial morphology in the HC or other brain regions that were assessed in 15 month old rats.

In previous studies we reported that ladostigil (1 mg/kg/day), a compound with anti-oxidant (Maruyama et al. 2003) and anti-inflammatory activity (Moradov et al. 2015), prevented the development of learning and memory deficits in aging male Wistar rats (Weinstock et al. 2011 2013). Its effect was associated with a reduction in microglial activation in the PC, CC and Fx, but not in the hippocampal CA1 region (CA1-HC). Microglial activation was assessed as the increase in per cent area of immunoreactivity measured with an antibody to CD11b (Weinstock, et al. 2013). Drug treatment was initiated at the age of 16 months, while the object recognition memory of the rats was slightly impaired and continued for 6 months until the majority of untreated rats showed clear spatial learning deficits in the MWM. Earlier unpublished findings in our laboratory confirmed those of others (Wyss et al. 2000) that spatial learning in the MWM of 16 month old rats, as measured by path length to escape platform, did not differ significantly from that of 6 month old adults. However, we found that it took six months of treatment with ladostigil (1 mg/kg/day) in 16 month old rats to restore their object recognition ability to that in young adults (Weinstock et al. 2013).

The microenvironment in different brain regions shows considerable diversity in its metabolism, neurotransmitter profile and in the microglial transcriptome (Olah et al. 2011; Eggen et al. 2013; Grabert et al. 2016). This may explain the differences in the morphology of microglia in grey matter, which have radially extending processes, from those in white matter, which have a bipolar arborization (Lawson et al. 1990). After activation, microglia in grey matter have a higher expression of CD11b and CD45, retracted processes and may assume an amoeboid appearance in some brain regions (Eyo and Wu 2013). In white matter, injury and aging result in thickening of microglial processes (Hanlon et al. 2017).

The aim of the current study was to see how aging affected detailed microglial morphology in brain regions associated with the integration of learning and memory and to determine which changes in microglial structure in each region correlated best with the learning deficits. We also made a comprehensive analysis of the expression profiles of immune and inflammation related genes in the adult (4–5 months old) and aged (22 months old) HC and PC by means of transcriptome RNA-seq, and determined the effect of chronic treatment with ladostigil on glial morphology and associated changes in gene expression. Previous studies in brains of humans and rodents reported an age related increase in expression of genes in the HC associated with inflammatory processes. These included genes related to complement and MHC class II (Cribbs et al. 2012; Masser et al. 2014; Ivanov et al., 2017; Pardo et al. 2017). We were unable to find reports of such changes in the PC.

Materials and Methods

Animals and their Treatment

Males of the Wistar strain aged 4–5, or 22 months of age were used. Half of the latter were treated with ladostigil (1 mg/kg/day) for 6 months from the age of 16 months and the remainder with drinking fluid according to the guidelines of the

Animal Ethics Committee of the Hebrew University # MD-13-13,808-2 and as described in (Weinstock et al. 2013).

Assessment of Spatial Memory

Spatial memory in 12 adult (aged 4–5 months), 14 aged, untreated and 14 aged rats treated with ladostigil (aged 22 months) was assessed in the Morris water maze (MWM) as described in (Weinstock et al. 2011). To begin each trial the rat was placed into the water facing the maze wall from one of four start positions, evenly spaced around the pool (N, S, E and W). These were chosen randomly for all rats at the beginning of each day. If the rats failed to find the escape platform within 120 s it was placed on it for 20 s and then removed from the pool. The rats were given two trials a day for 4 days between 9:00 and 13:00 h with an inter-trial interval of 15 min. Each trial was recorded by a digital camera connected to a tracking system. The swim speed, latency to reach escape platform and distance swam was measured by means of an automated video-tracking system (HVS, UK Ltd).

Histology

Four days after the completion of the spatial memory test, six adult controls, and eight each of untreated aged and those given ladostigil were anesthetized with sodium pentobarbitone, perfused transcardially with 0.02 M phosphate buffer saline, pH 7.4 at room temperature, followed by ice-cold 4% paraformaldehyde and 4% sucrose in 0.1 M phosphate buffered saline pH 7.4. For immuno-histochemical staining, coronal brain blocks were cut on a cryostat and sections 30 μm thick were collected floating as previously described (Shoham et al. 2007). Microglia were stained by incubation with mouse anti CD11b subunit of complement receptor-3 (CR3) (clone OX42 from Chemicon, USA) as described in Weinstock et al., (2011), and with rabbit anti-ionized calcium binding adaptor molecule 1 protein (Iba1). Sections were stained either singly with diaminobenzidine (DAB) or doubly, by fluorescent antibodies (Table 1).

Selection of Histological Variables to Correlate with Behavior

We determined whether aging alters the microglial structural substrate for potential interaction with neuronal elements in the PC (Weinstock et al. 2013) and CA1-HC (Min et al. 2009; Woodward et al. 2017). Such interaction is mediated by the tips of microglial processes (Tremblay et al. 2010). Studies with transgenic mice expressing a green fluorescent reporter protein demonstrated that microglial tips present either as "stick like" shapes in which their diameter is the same as the process stem, or as "bulbs", in which the process thickens to 2–4 times that of the stem and forms a rounded shape reminiscent of a light bulb (Tremblay 2010). In senescence accelerated mice, immunohistochemical staining with anti Iba1 showed a reduction in the number of microglial tips in hippocampus that preceded the emergence of learning deficits. This suggested a relation between the number of such tips and learning (Hasegawa-Ishii et al. 2011) that might also apply in normal aging in rats. The number of bulbs in microglial processes has been shown to be influenced by neuronal activity in an in vivo fish larvae model (Li et al. 2012) that depends on complement 3 protein expression (reviewed in Tremblay et al. 2010). We therefore used immunohistochemical staining of complement 3 receptor in order to visualize bulbs in our study. We sought a correlation between each tip subtype and spatial learning in the MWM. The data from these analyses were compared to the regional area fraction of immunoreactivity as described in Weinstock et al., (2013). In a pilot immunohistochemical study in rats aged 16 months we observed a mild increase in the area fraction (percent area immunoreactivity) of microglial complement 3 receptor (cd11b) in CA1-HC which together with the data of Griffin et al., (2006), provides support for some change in microglial morphology at this age even though it is probably less than at 22 months at which learning deficits are clearly seen.

We also performed a morphological analysis of microglial processes in the white matter (CC and Fx) in which microglia may not modulate information processing by contact with neuronal circuitry but are in a position to respond to diffusible

Table 1 Immunohistochemistry in a set of sections employing different fluorophores or diaminobenzidine as the final color product (bright field imaging)

Primary antibody	Source	Dilution	Secondary antibody	Dilution	Source	Strept- Avidin/ Extravidin	Source
Fluorescence							
Rabbit x Iba 1	Wako Japan	1:4000	Donk. x Rabbit biotin	1:400	Millipore AP182B	DyLight 488, green	Jackson 016480084
Mouse x CD11b	Millipore	1:1000	Gt x Mouse biotin	1:400	Sigma B0529	Cy3 Red,	Sigma S6402
Diaminobenzidine							Sigma D5637
Rabbit x Iba 1	Wako Japan	1:4000	Donk. x Rabbit biotin	1:400	Millipore AP182B	Extravidin peroxidase	Sigma E2886
Mouse x CD11b	Millipore CBL1512	1:1000	Goat x Mouse biotin	1:400	Sigma B0529	Extravidin peroxidase	Sigma E2886

substances such as ATP released from myelinated axons (reviewed in Fields 2008). These, together with adenosine, have been shown to modulate microglial activity (Haynes et al. 2006; Gyoneva et al. 2009). Our preliminary microscopic examination revealed that microglia do not appear with their entire outline in white matter but only as processes. Therefore, we measured thickness of microglial processes which has previously been shown to be associated with their activation (Jonas et al. 2012) and determined its relation to spatial learning.

Sampling Methods and Quantification of Microglia

Coronal sections were from anterior-posterior range of P2.3 to P3.3 mm from the bregma (Paxinos and Watson 1986) for PC and P3.14 to P3.8 mm from the bregma for dorsal HC. To quantify the spatial density of microglia, images of Iba1-DAB positive cells were acquired using Olympus 61 bright field microscope and 10x objective. Six fields were obtained from each PC and HC of every rat. In the HC, microglia were only counted in the CA1 *stratum radiatum*, in which we previously found age related changes (Weinstock, et al. 2011). The area of each field was 0.6 square mm. The number of microglia was determined by means of ImageJ particle analysis plugin and averaged across six fields for each rat.

To quantify spatial distribution of CD11b, both DAB-stained and fluorescent-stained sections were sampled. DAB images were acquired as described above for cell counts. Fluorescent confocal images were acquired by the Olympus FV-1000 confocal microscope (Olympus, Japan). The images were converted to gray scale and the threshold adjusted so that only specific staining was detected by the ImageJ analysis software. To obtain percent area of immunoreactivity, the total area above threshold was calculated and divided by the total area of the sampled field. To quantify morphological variables, images were obtained from Iba1-DAB and CD11b-DAB stained sections using Olympus 61 bright field microscope and 40x objective. Five fields were sampled from each region (PC, CA1-HC, CC and Fx) of each rat. Each field measured 219 × 219 μm. From each grey matter field, five microglial cells were chosen for analysis. Microglia were selected if they had a visible soma in the plane of focus and a dendritic tree that contained at least three major branches arising from the soma. A total of 25 cells were analyzed from each rat for each grey matter region. For white matter, fields were sampled from the midline laterally to the dorsal horn of the lateral ventricle. Images were processed using ImageJ to obtain percent area immunoreactivity and to measure the thickness of microglial processes.

Morphological Analyses in Microglia of Grey Matter

In the PC, images were captured from layers 4–5 and in the CA1-HC, from the *stratum radiatum*. The number of tips on the processes for each microglial cell was measured using ImageJ. Since Iba1 was expressed in the entire dendritic tree, it was used to count the total number of process tips, while CD11b, which was expressed most reliably in the bulbs, was used to count them.

Fluorescence Microscopy

Three additional sections were sampled for fluorescent double staining of CD11b and Iba1. By the use of a combination of a fluorescent antibody to CD11b and Iba1 in the grey matter areas, we were able to choose the optimal quantification method. We used a DAB stain for each antibody to quantify microglial process tips and bulbs since this was more reliable than with the fluorescent stains (Fig. 1). All assessments were made by an observer blind to the age and treatment of the rats.

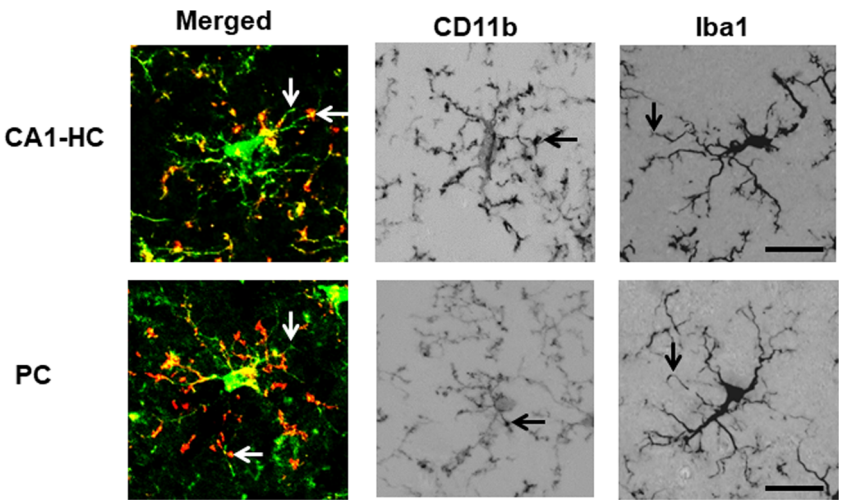

Fig. 1 Microglia in hippocampal CA1 region and parietal cortex (PC) stained with fluorescent antibodies and DAB to CD11b and Iba1. PC = Parietal cortex, CA1-HC = hippocampal CA1 region. Fluorescent double immunohistochemistry: CD11b, red; Iba1, green. Bright field DAB stain of CD11b and Iba1. Horizontal arrows indicate bulbs; vertical arrows indicate process tips. Calibration bar: 20 μM

Generation of Calibration Bars for Histological Figures

Confocal fluorescent or diaminobenzidine (DAB) images with a known size (e.g. 219 × 219 μm) were imported into a Power point composite figure. The Power point intrinsic ruler enabled determination of the length of ruler units that corresponded to the length in μm in the image. A line was drawn adjacent to the ruler to denote the length in μm.

Tissue Extraction and RNA Preparation

Six rats of each group were sacrificed three days after the spatial memory assessment, the whole brain was dissected and placed into chilled Hanks basal salt solution for less than three minutes. The HC and PC were dissected, weighed and placed in RNase-free labeled tubes that were immediately flash frozen and stored at −80 °C. RNA was isolated following the manufacturer's instructions (Qiagen, CA, USA). Qiagen RNeasy kit was used for tissue lysis. The reagent was added to the frozen tissue prior to homogenization. Approximately 500–800 ng of high-quality RNA was isolated per sample and tested for its purity.

Next Generation Sequencing

Transcriptome profile was determined for each animal and each sample of a brain area (HC and PC) by next generation sequencing pipeline (Trapnell et al. 2009). A RNA-seq library was prepared using a TruSeq RNA Sample Prep kit (Illumina, CA, USA). The sequencing was performed based on Illumina NextSeq550 platform with a 150 bp paired-end reads mode. On average, each sample produced 30–35 million reads. The sequencing protocol included sequence quality, removal of adaptor sequences (using FASTX- trim adaptor protocol) and removal of duplicated reads for minimized PCR amplification biases. Accepted fragments passed the FASTQ threshold and had ≤2 mismatch. The reads were aligned to the Rat genome (RGSC Rnor_6.0, 2014) using TopHat2. We used Cufflinks assembler that estimates gene abundances by FPKM (Fragments per Kilobase Million), and tests the differential expression in RNA-Seq sample groups. Based on Cufflinks toolkit (version 2.2.1) the relative abundances of the transcripts were estimated according to FPKM support. For statistical assessment of the counts, we applied DESeq2 functions. A minimal fold change threshold of 1.25, and a corrected mean p value of <0.05 were required for each pairs of groups. Total of 122 genes from HC and 196 from PC met the statistical criteria for ladostigil treated animals and their matched aged group (p value <0.05). Setting a threshold of FPKM = 20 for these gene sets resulted in 170 and 106 genes for PC and HC, respectively which were further analyzed.

Bioinformatic Analysis

Functional enrichment of gene lists was performed using the DAVID (Huang et al. 2007) platform based on annotations extracted from Gene Ontology (GO), UniProt and KEGG pathways. Statistical enrichment of gene lists was performed with respect to the gene expressed in the relevant brain area as reference sets. The number of identified expressed genes revealed by the RNA-seq protocol was 13,923 and 14,110 genes for HC and PC, respectively.

Statistics

Average daily path lengths swum by rats in the MWM during 4 days were analyzed by repeated Analysis of Variance (ANOVA); measures of microglial morphology were analyzed by ANOVA followed by Tukey's *post hoc* test. Significance of the correlations between performance in the MWM test and measures of microglial morphology was determined by student's t test. Data represent the means and standard error of the mean (SEM) for path length and mean and standard deviation (STD) for microglial analyses. A p value of <0.05 was considered to be significant.

Results

Spatial Learning

Since we found that the aged rats swam more slowly than the adult ones in this study we measured the differences in path length swam by the rats to reach the escape platform rather than latency as previously reported (Panarsky et al. 2012). In order to have a single number to correlate with different measures in microglia, we averaged path length over the last two days of the test for each rat. This was significantly greater for aged untreated than young adults. Ladostigil reduced the average path swam by the rats during the 3rd and 4th days (Fig. 2). The mean values obtained for the three groups were: young adults, 3.92 ± 0.44 m; aged untreated 13.06 ± 0.86 m ($p < 0.0001$, cf. adult controls); aged + ladostigil, 6.20 ± 0.86 m ($p < 0.00025$, cf. aged controls).

Analyses of Microglia in Different Brain Regions

As shown by others (Mouton et al. 2002; VanGuilder et al. 2011), the number of microglia in the CA1-HC and PC of aged rats did not differ from those in adult animals (Table 2). However, the area fraction occupied by microglia was significantly higher in aged than in adult rats in the PC, CA1-HC, CC and Fx (Fig. 3). Ladostigil treatment selectively reduced the area fraction in the PC ($p < 0.01$), CC ($p < 0.05$) but not in the CA1-HC or Fx (Fig. 3). There were significant

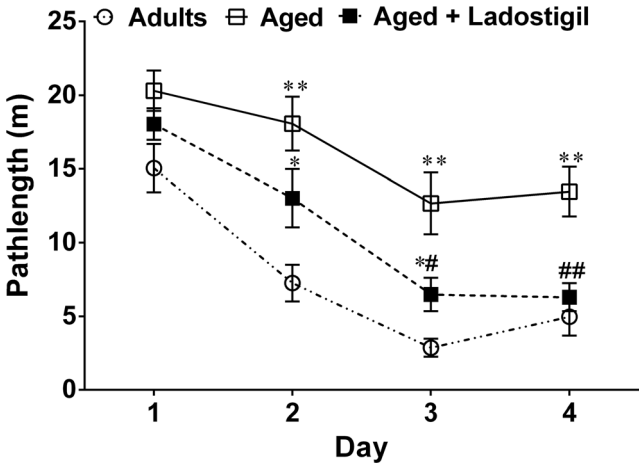

Fig. 2 Effect of ladostigil treatment on reference memory in the Morris water maze. Data show the mean ± SEM of path length to reach the escape platform as the average of two daily trials on four successive days in adult rats aged 4–5 months, aged rats aged 22 months, with and without ladostigil. Repeated measures ANOVA showed a significant effect of trial ($p < 0.0001$) and of group, ($p < 0.05$). Significantly different from adult control rats, * $p < 0.05$; ** $p < 0.01$); significantly different from untreated aged rats $^{\#}$ $p < 0.05$; $^{\#\#}$ $p < 0.01$)

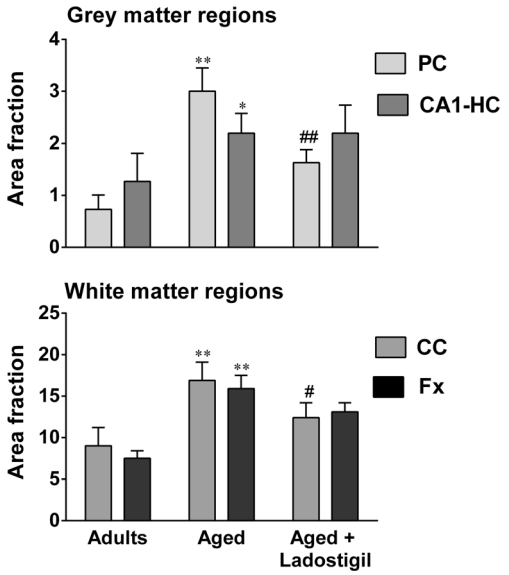

Fig. 3 Quantification of area fraction occupied by microglia in different brain regions. PC = Parietal cortex, CA1-HC = hippocampal CA1 region; CC = corpus callosum; Fx = fornix. ANOVA for area fraction was; PC: $F_{2,18} = 10.00$, $p < 0.001$; CA1-HC: $F_{2,18} = 1.14$, $p = 0.34$; CC: $F_{2,18} = 3.40$, $p < 0.05$; Fx: $F_{2,18} = 9.93$, $p < 0.001$. Significantly different from adult control rats, * $p < 0.05$; ** $p < 0.01$; significantly different from untreated aged rats $^{\#}$ $p < 0.05$; $^{\#\#}$ $p < 0.01$. Area fraction was significantly increased in the PC, CC and Fx of aged rats. Ladostigil reduced the area fraction significantly in the PC and CC

correlations between path length to escape platform and area fraction in the PC, $r = 0.52$, $p < 0.02$; CC, $r = 0.59$, $p < 0.01$ and Fx, $r = 0.63$, $p < 0.005$, but not in the CA1-HC.

In the CA1-HC of adult controls, CD11b expression was seen in bulbs found on some microglial processes, while Iba1 expression was apparent in the entire microglial outline except for bulbs (Fig. 4a). Bulbs stained for CD11b in 22 month aged rats were seen at the tips of many processes and also along their length. The number of bulbs was higher, and the number of processes lower than in adults (Fig. 4a, b). Ladostigil increased the number of bulbs and processes (Fig. 4a, b). A significant negative correlation was found between path length to escape platform (shorter distance) and the number of process tips in the CA1-HC, $r = 0.654$ $p < 0.005$ (Fig. 4c), but there was no significant correlation with the number of bulbs ($r = 0.317$) indicating that performance in spatial learning was increased in proportion to the number of processes.

Table 2 Microglia spatial distribution (DAB, Iba1)

Treatment Group	PC	CA1-HC
Young Adults	250.0 ± 26.3	224.2 ± 19.8
Aged, untreated	255.4 ± 23	227.4 ± 12.8
Aged + Ladostigil	237.4 ± 9.7	221.5 ± 14.0
ANOVA	NS	NS

Entries are mean numbers of microglial cells per square millimeters and the respective standard deviations

PC = parietal cortex, CA1-HC = hippocampal CA1 region, stratum radiatum

ANOVA for microglial spatial density was; PC: $F_{2,19} = 0.29$, $p < 0.75$; CA1-HC: $F_{2,19} = 1.63$, $p < 0.22$

In the PC, aging increased the number of bulbs ($p < 0.01$) and process tips ($p < 0.05$). In contrast to its action in the CA1-HC, ladostigil reduced the number of bulbs ($p < 0.01$), but increased the number of processes ($p < 0.01$) (Fig. 5a, b). A significant positive correlation was found between path length to escape platform and the number of bulbs in the PC, $r = 0.66$, $p < 0.005$ (Fig. 5c) but not with the number of process tips ($r = 0.102$), indicating that the larger the number of bulbs the less effective was their spatial learning.

In the CC of adult rats, most expression of CD11b and Iba1 was in the microglial processes. The area fraction of CD11b staining was significantly increased by aging (Table 3), as was the thickness of the processes (Fig. 6a, b). As in adult controls, CD11b, expression in aged rats was seen mainly in the processes but these were thicker. Some cell bodies in the CC were also more densely stained. Ladostigil prevented the increase in thickness of the processes in the CC ($p < 0.0001$) (Fig. 6 a, b). A significant positive correlation was found between path length to escape platform and thickness of the processes in the CC, $r = 0.755$ $p < 0.0001$ (Fig. 6c).

Expression of Microglial Associated Genes

In the gene analysis we focused on the effect of aging on differential expression of a number of microglial genes in the HC and PC because of their importance for microglial morphology and migration by activating membranous

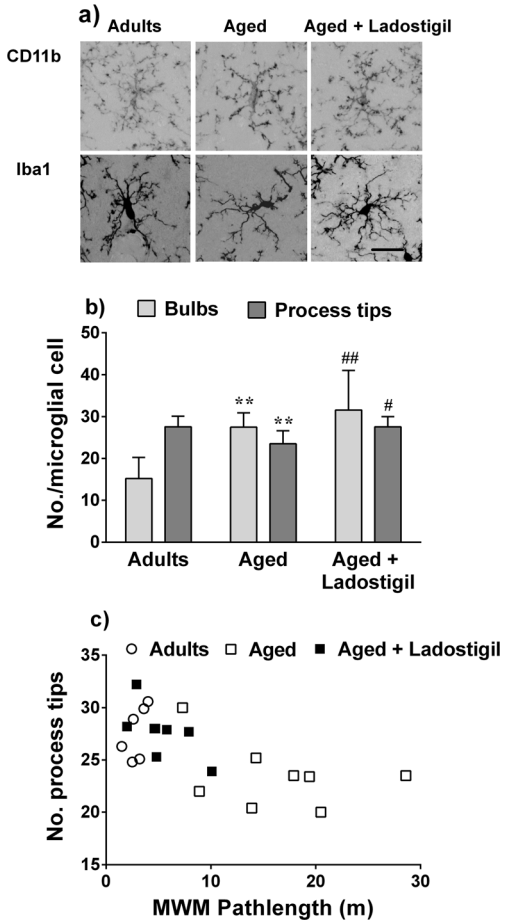

Fig. 4 Microglia in hippocampal CA1 (CA1-HC) region stained with CD11b and Iba1. **a** DAB stain used for quantification of bulbs and processes. Calibration bar: 20 μM. **b** Quantification of bulbs and process tips in CA1-HC. ANOVA for number of process tips/microglial cell, $F_{2,21} = 5.64$; $p < 0.02$, and for number of bulbs, $F_{2,21} = 14.24$, $p < 0.0002$. Significantly different from adult control rats, ** $p < 0.01$; significantly different from untreated aged rats, $^{\#}$ $p < 0.05$, $^{\#\#}$ $p < 0.01$. (**c**) Relation between number of processes in microglial cells in the CA1-HC and path length to escape platform, $r = -0.65$, $p < 0.005$. Aging increased the number of bulbs/cell in CA1-HC and decreased the number of processes. Ladostigil increased the number of bulbs and processes

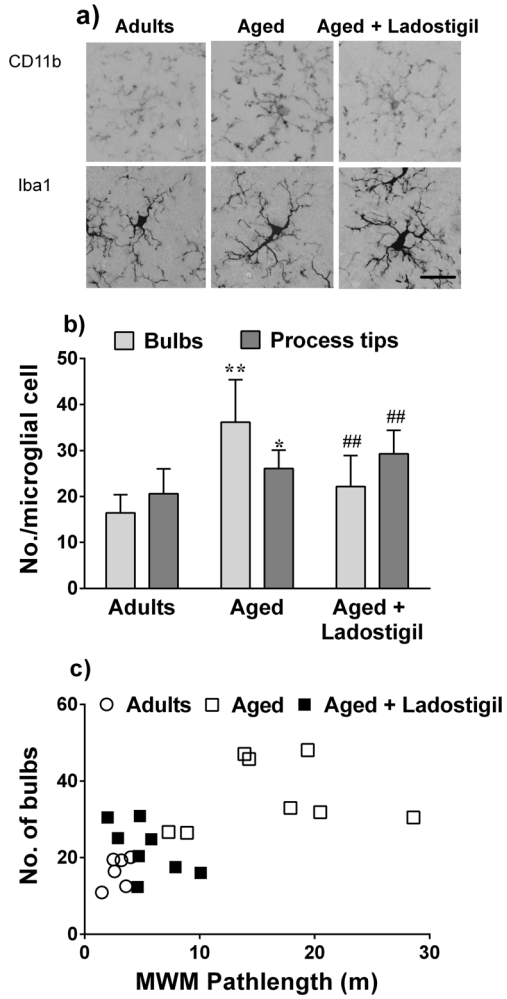

Fig. 5 Microglia in parietal cortex (PC) stained with CD11b and Iba1. **a** DAB stain used for quantification of bulbs and process tips. Calibration bar: 20 μM. **b** Quantification of bulbs and process tips in PC, ANOVA for number of process tips/microglial cell was $F_{2,21} = 5.64$; $p < 0.02$; number of bulbs, $F_{2,21} = 14.24$, $p < 0.0002$. Significantly different from adult control rats * $p < 0.05$; ** $p < 0.01$; significantly different from untreated aged rats, $^{\#\#}$ $p < 0.01$. Aging increased the numbers of bulbs/cell and processes. Ladostigil decreased the number of bulbs in the PC and increased the number of process tips. **c** Relation between number of microglial bulbs in PC and path length to escape platform, $r = 0.62$, $p < 0.005$

signaling (de Monasterio-Schrader et al. 2013; Hickman et al. 2013; Safaiyan et al. 2016; Galatro et al. 2017). Many representative MHC class II genes that are membrane recognition markers and are considered hallmarks of microglia in the aging rodent brain (Beutner et al. 2013; Grabert et al. 2016) were overexpressed in the HC of aging rats, compared to only four such genes in the PC (Table 3). Aging also significantly increased the expression of two purinergic receptors, A_{2A}R(Adora2a) and P2rx7R (a ligand gated ion channel) by 10 and 2 fold, respectively ($p < 0.0001$) in the HC, but not in the PC. Additionally, an age-induced enrichment in the expression of voltage-dependent K^+ channel (Kcnt1 and Kcnf1), Ca^{2+} channel (Cacna2d2) and Na^+ channel (Scn4b) genes was observed in the HC but not in the PC (Table 4).

In the PC, ladostigil significantly reduced the expression of the genes of the MHC class II that were up-regulated by aging (Table 3) and several of those associated with membrane lipid signaling which were unaffected by aging (Fig. 7). In the HC, the expression of only 4 of 16 MHC class II genes up regulated by aging were significantly altered by ladostigil; three were further increase and one, decreased. Ladostigil also completely prevented the increase in A_{2A} R expression ($p < 4e^{-14}$), but not that of P2rx7. Ladostigil had no effect on the expression of either purinergic receptor in the PC. Ladostigil reduced the expression of all genes associated with ion channels that were up-regulated by aging in the HC (Table 4). In the PC, ladostigil treatment significantly reduced

Table 3 Effect of aging and ladostigil treatment on expression of genes involved in immune activation in the parietal cortex and hippocampus

Gene	Gene name	Relative Expression		
		Adult	Aged	Ladostigil
Hippocampus				
RT1-A1	RT1 class Ia	10.6**	15.9	22.9
RT1-A2	RT1 class Ia	16.5***	25.9	33.8
RT1-A3	RT1 class I	5.8**	8.2	14.6
RT1-Ba	RT1 class II	2.8***	9.5	22.6*
RT1-Bb	RT1 class II	1.0*	2.5	13.5***
RT1-CE1	RT1 class I	4.8***	9.6	10.4
RT1-CE10	RT1 class I	6.9	9.7	14.7
RT1-CE2	RT1 class I	5.4*	8.6	11.6
RT1-CE3	RT1 class I	4.4*	7.6	9.1
RT1-CE5	RT1 class I	14.4**	21.2	27.2
RT1-CE7	RT1 class I	8.4***	15.5	20.9
RT1-Da	RT1 class II	4.7***	21.8	44.1*
RT1-Db1	RT1 class II	2.9***	11.6	20.0
RT1-M6–1	RT1 class I	6.9*	9.9	13.1
RT1-N2	RT1 class Ib	12.6	10.2	5.3**
RT1-S3	RT1 class Ib	6.9***	14.3	20.5
Parietal cortex				
Ttr	transthyretin(Ttr)	15.3***	220.2	54.7***
RT1-Db1	RT1 class II, locus Db1(RT1-Db1)	0.7***	9.1	4.0*
RT1-Da	RT1 class II, locus Da(RT1-Da)	2.3***	20.2	9.0**
Cd74	CD74 molecule(Cd74)	6.8***	63.4	31.3**

Significantly different from aged, *$p < 0.05$; **$p < 0.005$; ***$p < 0.0005$

the expression of several K^+, Ca^{2+} and Na^+ channels even though they were unaffected by aging (Table 5).

Discussion

A novel feature of the current study was that it examined the effect of aging on the morphology of microglia in four different regions in the rat brain that are associated with control of spatial memory and found that this differed in each region. In the CA1-HC, we confirmed that aging caused retraction and thickening of the processes (Flanary et al. 2007; VanGuilder et al. 2011), reduced the number of their branches, as reported by others (von Bernhardi et al. 2010; Hasegawa-Ishii et al. 2011) but increased the number of bulbs. However, in the PC, aging increased the number of process tips, the area fraction stained for CD11b, a marker of microglial activation (Eggen et al. 2013) and the number of bulbs. In white matter regions of the Fx and CC, microglia are aligned horizontally along the white matter tracts and their branches are not all visible in each cell. Aging increased the thickness of the processes, enlarged their soma and the area stained by CD11b, testifying to increased activation.

Treatment from the age of 16 months for 6 months with ladostigil (1 mg/kg/day) also influenced microglial morphology in an area-specific manner. In the CA1-HC and PC, ladostigil significantly increased the number of process tips, but in the CA1-HC it increased the number of bulbs while reducing them in the PC. Ladostigil also reduced the thickness of processes in the white matter regions. In the CA1-HC, the distance to escape platform was inversely correlated with the number of processes, but showed no correlation positive or negative with the number of bulbs. In the PC, the distance to escape platform was positively correlated with the number of bulbs and in the CC and Fx, with the thickness of processes.

VanGuilder et al., (2011) failed to find a relation between memory and the total increase in Iba1 protein in the different rat hippocampal regions because this measure reflects microglial cellular hypertrophy, which occurred in all aged rats irrespective of their cognitive ability. Furthermore, they were also unable to relate cognition to percent of activated microglia in different sub regions of the HC. On the other hand, Hovens et al., (2015) found an increase in the ratio of cell body to cell size in the dentate gyrus and CA3 HC region in aged rats, which also indicates retraction of processes. However, unlike

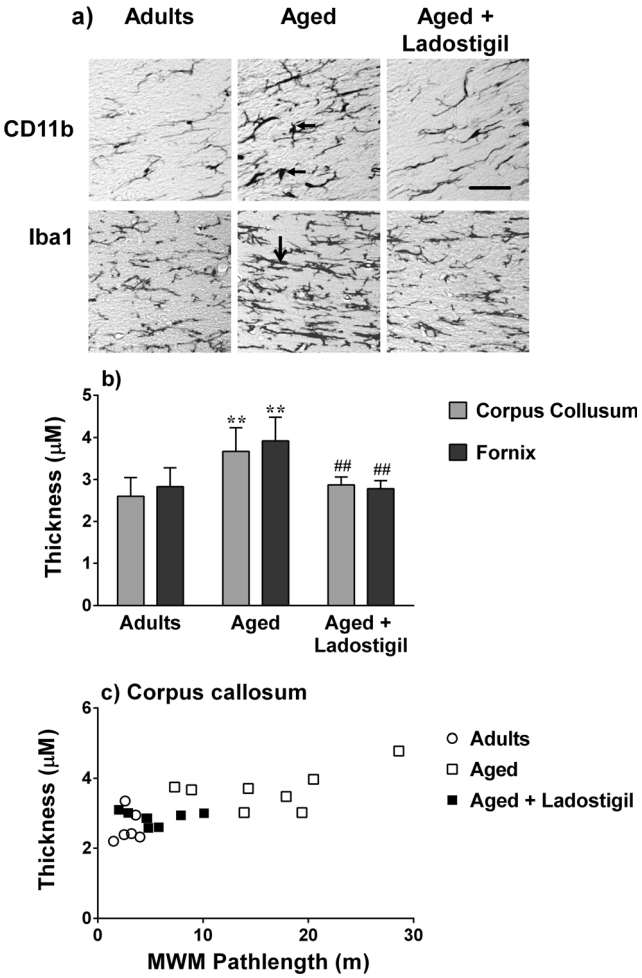

Fig. 6 Microglia in the corpus callosum (CC) stained with antibody to CD11b and Iba1. **a** DAB stain of processes in white matter regions (CC and Fx). Vertical arrow indicates thickened process in aged rat. Horizontal arrow indicates enlarged soma. Calibration bar: 20 μM. **b** Quantification of processes in CC and Fx. ANOVA for thickness of microglial processes in the CC, $F_{2,19} = 12.41$, $p < 0.0005$ and Fx, $F_{2,19} = 19{:}61$, $p < 0.0005$. Significantly different from adult control rats ** $p < 0.01$; significantly different from untreated aged rats ## $p < 0.01$. Ladostigil prevented the thickening of the processes induced by aging. **c**) Relation between thickness of processes in CC and path length to escape platform, $r = 0.75$, $p < 0.0001$

in the current study, this measure was significantly correlated with memory retention but not with learning in the MWM.

Like the differential effect of aging on microglial morphology in the HC and PC there were also differences in expression of different classes of genes in these brain areas. Aging caused a significant increase in the expression of 14 genes of the MHC class II in the HC, which are associated with microglial priming (Norden and Godbout 2013) but only of four such genes in the PC. There was also a selective 10-fold increase in the HC in the expression of $A_{2A}R$ and a moderate increase in expression of $P2Y_{12}R$ (30%, $p = 0.05$) but not in the PC. Brain inflammation and neuronal injury release ATP that activates microglia causing them either to retract their processes adopting an amoeboid morphology, or to extend them depending on the receptor activated (Orr et al. 2009). Stimulation of the A_{2A} R by extracellular adenosine results in process retraction (Haynes et al. 2006). Although we did not measure the length of processes in the CA1-HC, it can clearly be seen that microglia in this brain area, but not in the PC, have shorter processes in the aged rat (Fig. 4), together with a decrease in their number. Thus, our findings of an increased expression of $A_{2A}R$ and reduction in the number of processes in CA1-HC results in an impairment in their ability to survey the micro environment and respond to changes in neuronal activity. They also indicate that in this area the potential for surveying the neuronal environment constitutes the significant limiting factor on spatial performance rather than the state of activation.

There was also a significant increase in the expression of several ion channel genes in the aged HC which did not occur in the PC. The expression of ion channels in microglia determines their functions like migration (Schwab et al. 2012), morphology, activation and secretion of proinflammatory cytokines (Visentin et al. 1995; Stebbing et al. 2015). Thus, it has been shown that exposure of microglia to amyloid peptide results in translocation of intracellular Cl^- and Ca^{2+} activated K^+ channels, while blocking the Cl^- channel increases protection from neurotoxicity caused by oxidative stress (Skaper 2011).

Ladostigil treatment had a differential effect on gene expression in the two brain areas. In keeping with the increase in the number of processes in the HC, which also appeared to be longer in ladostigil treated rats, the expression of $A_{2A}R$ was significantly reduced (4.2 fold, $p = 3.75^{\text{e-14}}$). This suggests

Table 4 Effect of aging and ladostigil treatment on the gene expression of ion channels in the hippocampus

			Relative Expression		
Conducting ion	Gene id	Function	Adult	Aged	Ladostigil
Potassium	Kcnt1	Calcium activated	11.62***	22.28	13.20***
Potassium	Kcnf1	Modifier/silencer	13.13*	17.43	12.13*
Sodium	Scn4b	Beta unit-type 4	11.82***	21.16	16.52*
Calcium	Cacna2d2	Alpha2-delta unit	5.51***	12.34	7.70*
Chloride	Glra2	Glycine gated	6.40**	9.30	6.08*
Cation	Trpm3	Transient potential	10.97***	21.88	16.26***

Significantly different from aged, *$p < 0.05$; **$p < 0.005$; ***$p < 0.0005$

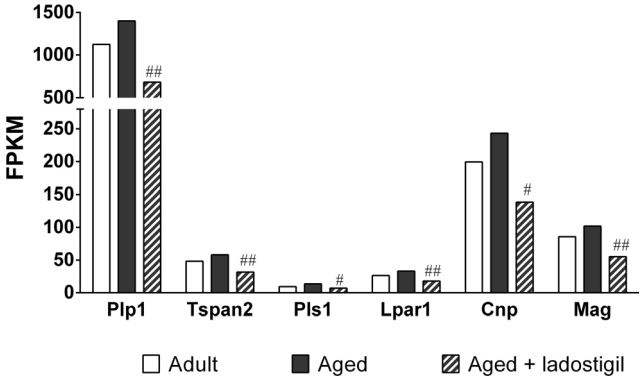

Fig. 7 Effect of age and ladostigil treatment on gene expression in the parietal cortex as quantified by RNA-Seq. Each group composed of an average of RNA-Seq data collected from ≥3 animals and normalized by FPKM (Fragments per kilobase million). Data show expression of genes in PC of adult, aged untreated, and aged rats given ladostigil. Significantly different from untreated aged rats, $^{\#}p < 0.05$, $^{\#\#}p < 0.01$

that together with its effects on purinergic receptors in the HC, ladostigil may improve contact between microglia and neuronal elements. On the other hand, ladostigil further increased the expression of 3 genes involved in immune activation, in contrast to its effect in the PC in which their expression was reduced. This finding is in keeping with the increase in the number of bulbs in the CA1-HC but a decrease in the PC. Also in the PC, ladostigil treatment decreased the expression of several genes associated with ion channels and genes that control microglial morphology and migration by activating membranous signaling, even though these genes were not significantly altered by aging. The latter genes include, Plp that codes for the proteolipid protein, which is a major membrane protein component in myelin; Pls1 (also called Plscr1), that participates in migration of phospholipids upon binding calcium ions and plays a role in recognition of apoptotic and injured cells; Tspan2, Mag and Lpar1, that are active in cell adhesion and motility in the brain (Yaseen et al. 2017) and are involved in triggering inflammation in response to stimuli. Cnp (also called CNPase) that is among the most abundant proteins in CNS myelin. In this way ladostigil also improves activity between microglia and neuronal elements in the PC.

Increase in microglial thickness in white matter has also been reported in the aging brain of primates in which adjacent microglia engulf myelin debris (Peters et al. 2010). Microglial activation may contribute to myelin damage by exacerbating oxidative and nitrative stress (Smith et al. 1999). Further support for a role of inflammation in myelin damage is found in thickened processes in the CC after head injury, which also results in spatial memory impairment and can be prevented by treatment with the anti-inflammatory agent, minocycline (Hanlon et al. 2017). In the CC and Fx ladostigil prevented the microglial alteration and process thickening, which was inversely correlated to spatial learning.

At the descriptive level, the present results suggest that local signals may modulate features of microglial morphology that differ according to the brain region. Only some of the features correlate with spatial learning and these appear to be area specific. Likewise, while ladostigil causes significant alterations in microglial morphology in all areas examined, its effect on gene expression associated with microglial activation is also area specific.

Conclusions

The study shows for the first time that morphological alterations in microglia induced by age and chronic treatment with ladostigil, differ in several brain areas involved in the

Table 5 Effect of aging and ladostigil treatment on the gene expression of ion channels in the parietal cortex

			Relative Expression		
Conducting ion	Gene_id	Function	Adult	Aged	Ladostigil
Potassium	Kcnc2	Delayed rectifier	47.09	53.13	38.37*
Potassium	Kcnq5l	Delayed rectifier	43.65	47.78	29.73*
Potassium	Kcnc1	Delayed rectifier	42.19	49.52	28.88*
Potassium	Kcna1	Delayed rectifier	40.06	40.88	23.30*
Potassium	Kcnab3	Beta subunit	28.92	26.68	11.31***
Potassium	Kcns1	Modifier/silencer	25.16	23.09	7.17***
Potassium	Kcnh7	Inwardly-rectifying	17.59	19.69	11.48*
Potassium	Kctd8	Tetramerisation domain	11.91	10.54	5.71*
Potassium	Kcnh5	Outward-rectifying	9.58	9.35	4.92*
Sodium	Scn1a	Type 1	75.88	74.32	39.67*
Sodium	Scn1b	Type 2	563.8	560.3	289.3**
Sodium	Scn4b	Beta unit-type 4	73.26	71.65	23.30***

There was no significant differences in gene expression of any channels between adult and aged rats. Significantly different from aged, $^{*}p < 0.05$; $^{**}p < 0.005$; $^{***}p < 0.0005$

mediation of spatial learning in rats. We also show a significant correlation between spatial learning, age and drug-induced alterations in microglial morphology that are seen in a given brain area. The specific alterations in glial morphology in the CA1-HC and PC are supported by changes in region dependent gene expression.

Acknowledgements We gratefully acknowledge the help given by Netanel Dwolatzky, Ayelet Gottstein and Coral Haddad in performing the microglial measurements, Tsiona Eliyahu for RNA preparation for sequencing and Amos Stern for data analysis.

Funding This research did not receive any specific grant from funding agencies in the public, commercial, or not-for-profit sectors, but was supported by research funds of MW at the Hebrew University.

Compliance with Ethical Standards

Conflicts of Interest The authors declare no conflict of interest.

References

Aggleton JP, Poirier GL, Aggleton HS, Vann SD, Pearce JM (2009) Lesions of the fornix and anterior thalamic nuclei dissociate different aspects of hippocampal-dependent spatial learning: implications for the neural basis of scene learning. Behav Neurosci 123:504–519

Albasser MM, Dumont JR, Amin E, Holmes JD, Horne MR, Pearce JM, Aggleton JP (2013) Association rules for rat spatial learning: the importance of the hippocampus for binding item identity with item location. Hippocampus 23:1162–1178

Bettcher BM, Watson CL, Walsh CM, Lobach IV, Neuhaus J, Miller JW, Green R, Patel N, Dutt S, Busovaca E, Rosen HJ, Yaffe K, Miller BL, Kramer JH (2014) Interleukin-6, age, and corpus callosum integrity. PLoS One 9:e106521

Beutner C, Linnartz-Gerlach B, Schmidt SV, Beyer M, Mallmann MR, Staratschek-Jox A, Schultze JL, Neumann H (2013) Unique transcriptome signature of mouse microglia. Glia 61:1429–1442

Bickford PC, Flowers A, Grimmig B (2017) Aging leads to altered microglial function that reduces brain resiliency increasing vulnerability to neurodegenerative diseases. Exp Gerontol 94:4–8

Conejo NM, Cimadevilla JM, Gonzalez-Pardo H, Mendez-Couz M, Arias JL (2013) Hippocampal inactivation with TTX impairs long-term spatial memory retrieval and modifies brain metabolic activity. PLoS One 8:e64749

Cribbs DH, Berchtold NC, Perreau V, Coleman PD, Rogers J, Tenner AJ, Cotman CW (2012) Extensive innate immune gene activation accompanies brain aging, increasing vulnerability to cognitive decline and neurodegeneration: a microarray study. J Neuroinflammation 9:179

de Monasterio-Schrader P, Patzig J, Mobius W, Barrette B, Wagner TL, Kusch K, Edgar JM, Brophy PJ, Werner HB (2013) Uncoupling of neuroinflammation from axonal degeneration in mice lacking the myelin protein tetraspanin-2. Glia 61:1832–1847

Eggen BJ, Raj D, Hanisch UK, Boddeke HW (2013) Microglial phenotype and adaptation. J NeuroImmune Pharmacol 8:807–823

Eyo UB, Wu LJ (2013) Bidirectional microglia-neuron communication in the healthy brain. Neural Plast 2013:456857

Fields RD (2008) White matter in learning, cognition and psychiatric disorders. Trends Neurosci 31:361–370

Flanary BE, Sammons NW, Nguyen C, Walker D, Streit WJ (2007) Evidence that aging and amyloid promote microglial cell senescence. Rejuvenation Res 10:61–74

Galatro TF, Holtman IR, Lerario AM, Vainchtein ID, Brouwer N, Sola PR, Veras MM, Pereira TF, Leite REP, Moller T, Wes PD, Sogayar MC, Laman JD, den Dunnen W, Pasqualucci CA, Oba-Shinjo SM, Boddeke E, Marie SKN, Eggen BJL (2017) Transcriptomic analysis of purified human cortical microglia reveals age-associated changes. Nat Neurosci 20:1162–1171

Gallagher M, Nicolle MM (1993) Animal models of normal aging: relationship between cognitive decline and markers in hippocampal circuitry. Behav Brain Res 57:155–162

Grabert K, Michoel T, Karavolos MH, Clohisey S, Baillie JK, Stevens MP, Freeman TC, Summers KM, McColl BW (2016) Microglial brain region-dependent diversity and selective regional sensitivities to aging. Nat Neurosci 19:504–516

Griffin R, Nally R, Nolan Y, McCartney Y, Linden J, Lynch MA (2006) The age-related attenuation in long-term potentiation is associated with microglial activation. J Neurochem 99:1263–1272

Gyoneva S, Orr AG, Traynelis SF (2009) Differential regulation of microglial motility by ATP/ADP and adenosine. Parkinsonism Relat Disord 15(Suppl 3):S195–S199

Hanlon LA, Raghupathi R, Huh JW (2017) Differential effects of minocycline on microglial activation and neurodegeneration following closed head injury in the neonate rat. Exp Neurol 290:1–14

Hasegawa-Ishii S, Takei S, Chiba Y, Furukawa A, Umegaki H, Iguchi A, Kawamura N, Yoshikawa K, Hosokawa M, Shimada A (2011) Morphological impairments in microglia precede age-related neuronal degeneration in senescence-accelerated mice. Neuropathology 31:20–28

Haynes SE, Hollopeter G, Yang G, Kurpius D, Dailey ME, Gan WB, Julius D (2006) The P2Y12 receptor regulates microglial activation by extracellular nucleotides. Nat Neurosci 9:1512–1519

Hebda-Bauer EK, Morano MI, Therrien B (1999) Aging and corticosterone injections affect spatial learning in Fischer-344 X Brown Norway rats. Brain Res 827:93–103

Hescham S, Lim LW, Jahanshahi A, Steinbusch HW, Prickaerts J, Blokland A, Temel Y (2013) Deep brain stimulation of the forniceal area enhances memory functions in experimental dementia: the role of stimulation parameters. Brain Stimul 6:72–77

Hickman SE, Kingery ND, Ohsumi TK, Borowsky ML, Wang LC, Means TK, El Khoury J (2013) The microglial sensome revealed by direct RNA sequencing. Nat Neurosci 16:1896–1905

Hovens IB, van Leeuwen BL, Nyakas C, Heineman E, van der Zee EA, Schoemaker RG (2015) Postoperative cognitive dysfunction and microglial activation in associated brain regions in old rats. Neurobiol Learn Mem 118:74–79

Huang DW, Sherman BT, Tan Q, Collins JR, Alvord WG, Roayaei J, Stephens R, Baseler MW, Lane HC, Lempicki RA (2007) The DAVID gene functional classification tool: a novel biological module-centric algorithm to functionally analyze large gene lists. Genome Biol 8:R183

Ingram DK, Spangler EL, Iijima S, Ikari H, Kuo H, Greig NH, London ED (1994) Rodent models of memory dysfunction in Alzheimer's disease and normal aging: moving beyond the cholinergic hypothesis. Life Sci 55:2037–2049

Jacobson L, Zhang R, Elliffe D, Chen KF, Mathai S, McCarthy D, Waldvogel H, Guan J (2008) Correlation of cellular changes and spatial memory during aging in rats. Exp Gerontol 43:929–938

Jonas RA, Yuan TF, Liang YX, Jonas JB, Tay DK, Ellis-Behnke RG (2012) The spider effect: morphological and orienting classification of microglia in response to stimuli in vivo. PLoS One 7:e30763

Lana D, Iovino L, Nosi D, Wenk GL, Giovannini MG (2016) The neuron-astrocyte-microglia triad involvement in neuroinflammaging mechanisms in the CA3 hippocampus of memory-impaired aged rats. Exp Gerontol 83:71–88

Lawson LJ, Perry VH, Dri P, Gordon S (1990) Heterogeneity in the distribution and morphology of microglia in the normal adult mouse brain. Neuroscience 39:151–170

Li W, Muftuler LT, Chen G, Ward BD, Budde MD, Jones JL, Franczak MB, Antuono PG, Li SJ, Goveas JS (2014) Effects of the coexistence of late-life depression and mild cognitive impairment on white matter microstructure. J Neurol Sci 338:46–56

Li Y, Du XF, Liu CS, Wen ZL, Du JL (2012) Reciprocal regulation between resting microglial dynamics and neuronal activity in vivo. Dev Cell 23:1189–1202

Light LL, Zelinski EM (1983) Memory for spatial information in young and old adults. Dev Psychol 19:901–906

Maruyama W, Weinstock M, Youdim MB, Nagai M, Naoi M (2003) Anti-apoptotic action of anti-Alzheimer drug, TV3326 [(N-propargyl)-(3R)-aminoindan-5-yl]-ethyl methyl carbamate, a novel cholinesterase-monoamine oxidase inhibitor. Neurosci Lett 341: 233–236

Masser DR, Bixler GV, Brucklacher RM, Yan H, Giles CB, Wren JD, Sonntag WE, Freeman WM (2014) Hippocampal subregions exhibit both distinct and shared transcriptomic responses to aging and nonneurodegenerative cognitive decline. J Gerontol A Biol Sci Med Sci 69:1311–1324

McQuail JA, Nicolle MM (2015) Spatial reference memory in normal aging Fischer 344 x Brown Norway F1 hybrid rats. Neurobiol Aging 36:323–333

Min SS, Quan HY, Ma J, Han JS, Jeon BH, Seol GH (2009) Chronic brain inflammation impairs two forms of long-term potentiation in the rat hippocampal CA1 area. Neurosci Lett 456:20–24

Moradov D, Finkin-Groner E, Bejar C, Sunita P, Schorer-Apelbaum D, Barasch D, Nemirovski A, Cohen M, Weinstock M (2015) Dose-limiting inhibition of acetylcholinesterase by ladostigil results from the rapid formation and fast hydrolysis of the drug-enzyme complex formed by its major metabolite, R-MCPAI. Biochem Pharmacol 94: 164–172

Mouton PR, Long JM, Lei DL, Howard V, Jucker M, Calhoun ME, Ingram DK (2002) Age and gender effects on microglia and astrocyte numbers in brains of mice. Brain Res 956:30–35

Norden DM, Godbout JP (2013) Review: microglia of the aged brain: primed to be activated and resistant to regulation. Neuropathol Appl Neurobiol 39:19–34

Olah M, Biber K, Vinet J, Boddeke HW (2011) Microglia phenotype diversity. CNS Neurol Disord Drug Targets 10:108–118

Orr AG, Orr AL, Li XJ, Gross RE, Traynelis SF (2009) Adenosine a(2A) receptor mediates microglial process retraction. Nat Neurosci 12: 872–878

Panarsky R, Luques L, Weinstock M (2012) Anti-inflammatory effects of ladostigil and its metabolites in aged rat brain and in microglial cells. J NeuroImmune Pharmacol 7:488–498

Pardo J, Abba MC, Lacunza E, Francelle L, Morel GR, Outeiro TF, Goya RG (2017) Identification of a conserved gene signature associated with an exacerbated inflammatory environment in the hippocampus of aging rats. Hippocampus 27:435–449

Paxinos G, Watson C (1986) The rat brain in stereotaxic coordinates, 2nd edn. Academic Press, San Diego

Perry VH, Nicoll JA, Holmes C (2010) Microglia in neurodegenerative disease. Nat Rev Neurol 6:193–201

Peters A, Sethares C, Moss MB (2010) How the primate fornix is affected by age. J Comp Neurol 518:3962–3980

Petersen RC, Smith G, Kokmen E, Ivnik RJ, Tangalos EG (1992) Memory function in normal aging. Neurology 42:396–401

Pezdek K (1983) Memory for items and their spatial locations by young and elderly adults. Dev Psychobiol 19:895–900

Safaiyan S, Kannaiyan N, Snaidero N, Brioschi S, Biber K, Yona S, Edinger AL, Jung S, Rossner MJ, Simons M (2016) Age-related myelin degradation burdens the clearance function of microglia during aging. Nat Neurosci 19:995–998

Save E, Poucet B (2009) Role of the parietal cortex in long-term representation of spatial information in the rat. Neurobiol Learn Mem 91: 172–178

Schwab A, Fabian A, Hanley PJ, Stock C (2012) Role of ion channels and transporters in cell migration. Physiol Rev 92:1865–1913

Shoham S, Bejar C, Kovalev E, Schorer-Apelbaum D, Weinstock M (2007) Ladostigil prevents gliosis, oxidative-nitrative stress and memory deficits induced by intracerebroventricular injection of streptozotocin in rats. Neuropharmacology 52:836–843

Skaper SD (2011) Ion channels on microglia: therapeutic targets for neuroprotection. CNS Neurol Disord Drug Targets 10:44–56

Smith KJ, Kapoor R, Felts PA (1999) Demyelination: the role of reactive oxygen and nitrogen species. Brain Pathol 9:69–92

Stebbing MJ, Cottee JM, Rana I (2015) The role of ion channels in microglial activation and proliferation - a complex interplay between ligand-gated ion channels, K(+) channels, and intracellular ca(2.). Front Immunol 6:497

Trapnell C, Pachter L, Salzberg SL (2009) TopHat: discovering splice junctions with RNA-Seq. Bioinformatics 25:1105–1111

Tremblay ME, Lowery RL, Majewska AK (2010) Microglial interactions with synapses are modulated by visual experience. PLoS Biol 8: e1000527

Turturro A, Witt WW, Lewis S, Hass BS, Lipman RD, Hart RW (1999) Growth curves and survival characteristics of the animals used in the biomarkers of aging program. J Gerontol A Biol Sci Med Sci 54: B492–B501

VanGuilder HD, Bixler GV, Brucklacher RM, Farley JA, Yan H, Warrington JP, Sonntag WE, Freeman WM (2011) Concurrent hippocampal induction of MHC II pathway components and glial activation with advanced aging is not correlated with cognitive impairment. J Neuroinflammation 8:138

Vann SD, Erichsen JT, O'Mara SM, Aggleton JP (2011) Selective disconnection of the hippocampal formation projections to the mammillary bodies produces only mild deficits on spatial memory tasks: implications for fornix function. Hippocampus 21:945–957

von Bernhardi R, Tichauer JE, Eugenin J (2010) Aging-dependent changes of microglial cells and their relevance for neurodegenerative disorders. J Neurochem 112:1099–1114

Weinstock M, Luques L, Poltyrev T, Bejar C, Shoham S (2011) Ladostigil prevents age-related glial activation and spatial memory deficits in rats. Neurobiol Aging 32:1069–1078

Weinstock M, Bejar C, Schorer-Apelbaum D, Panarsky R, Luques L, Shoham S (2013) Dose-dependent effects of ladostigil on microglial activation and cognition in aged rats. J NeuroImmune Pharmacol 8: 345–355

Whitlock JR (2014) Navigating actions through the rodent parietal cortex. Front Hum Neurosci 8:293

Wong WT (2013) Microglial aging in the healthy CNS: phenotypes, drivers, and rejuvenation. Front Cell Neurosci 7:22

Woodward NC, Pakbin P, Saffari A, Shirmohammadi F, Haghani A, Sioutas C, Cacciottolo M, Morgan TE, Finch CE (2017) Traffic-related air pollution impact on mouse brain accelerates myelin and neuritic aging changes with specificity for CA1 neurons. Neurobiol Aging 53:48–58

Visentin S, Agresti C, Patrizio M, Levi G (1995) Ion channels in rat microglia and their different sensitivity to lipopolysaccharide and interferon-gamma. J Neurosci Res 42:439–451

Wyss JM, Chambless BD, Kadish I, van Groen T (2000) Age-related decline in water maze learning and memory in rats: strain differences. Neurobiol Aging 21:671–681

Yaseen IH, Monk PN, Partridge LJ (2017) Tspan2: a tetraspanin protein involved in oligodendrogenesis and cancer metastasis. Biochem Soc Trans 45:465–475